Theoretical Study on Reaction Mechanism of Fulminic Acid HCNO with CN Radical

Jing-Lin Pang,[†] Hong-Bin Xie,[†] Shao-Wen Zhang,[‡] Yi-Hong Ding,*[,†] and Ao-Qing Tang[†]

State Key Laboratory of Theoretical and Computational Chemistry, Institute of Theoretical Chemistry, Jilin University, Changchun 130023, and Department of Chemistry, College of Science, Beijing Institute of Technology, Beijing 100081, People's Republic of China

Received: October 3, 2007; Revised Manuscript Received: February 26, 2008

The HCNO + CN reaction is one potentially important process during the NO-reburning process for the reduction of NO*x* pollutants from fossil fuel combustion emissions. To compare with the recent experimental study, we performed the first theoretical potential energy surface investigation on the mechanism of HCNO + CN at the G3B3 and CCSD(T)/aug-cc-pVTZ levels based on the B3LYP/6-311++G(d,p) structures, covering various entrance, isomerization, and decomposition channels. The results indicate that the most favorable channel is to barrierlessly form the entrance isomer **L1c** NCCHNO followed by successive ring closure and concerted CC and NO bond rupture to generate the product **P1** HCN + NCO. However, the formation of **P4** ^{3}HCCN + NO, predicted as the only major product in the recent experiment, is kinetically much less competitive. This conclusion is further supported by the master equation rate constant calculation. Future experimental reinvestigations are strongly desired to test the newly predicted mechanism for the CN + HCNO reaction. Implications of the present results are discussed.

1. Introduction

Recently, fulminic acid (HCNO) has been identified as an important intermediate in the NO-reburning process for the reduction of NO*x* pollutants from fossil fuel combustion emissions.[1] Knowledge of the subsequent chemistry of HCNO should be of great interest in the overall NO-reburning mechanism. Up to now, several HCNO reactions have been investigated either experimentally[2–4] or theoretically.[1,5–7] One of these reactions is one between HCNO and the CN radical, which is an important species in NO*x* formation mechanisms in both fuel-rich hydrocarbon flames and flames containing fuel nitrogen.[8–10] In 2006, Feng and Hershberger performed an experimental study on the kinetics of HCNO + CN and found it to be fast with a total rate constant of $(1.04 \pm 0.1) \times 10^{-10}$ cm^3 molecules^{-1} s^{-1} at 298 K.[2] On the basis of the detection of NO and consideration of various secondary reactions, they concluded that the formation of ^{3}HCCN + NO was the only major product channel. They thus speculated a simple mechanism, that is,

$$\mathrm{HCNO + CN \rightarrow NCCHNO \rightarrow HCCN + NO} \qquad \text{(Scheme 1a)}$$

Also, they said that "...our experimental results suggest that other pathways are higher in energy and are not significant." That is to say, the formation of other product channels is unlikely. To the best of our knowledge, there is hitherto no theoretical study on the mechanism of HCNO + CN.

However, it seems somewhat puzzling when we compare the proposed mechanism of HCNO + CN with that of another fast ^{3}HCCN + NO reaction. For the ^{3}HCCN + NO reaction, both the experimental[11] and the theoretical studies[12] have indicated that the major product channel is

$$\mathrm{^3HCCN + NO \rightarrow NCCHNO \rightarrow N\text{-}cCONCH \rightarrow HCN + NCO} \qquad \text{(Scheme 1b)}$$

Because all of the intermediates and transition states lie lower than ^{3}HCCN + NO, simply from the potential energy surface (PES) information, we might say that the most favorable evolution fate of NCCHNO is decomposition to HCN + NCO instead of ^{3}HCCN + NO. If the HCNO + CN reaction indeed proceeds via the intermediate NCCHNO (Scheme 1a), as speculated by Feng and Hershberger,[2] the eventual product could be HCN + NCO rather than ^{3}HCCN + NO concerning the PES. On the other hand, we are aware that in dynamics, distribution of the final products may also depend on the energy available to the system. So, a combined PES and dynamic study of the title reaction is desirable. The former can present detailed isomerization and dissociation pathways starting from the reactant HCNO + CN, while the latter can provide a quantitative description of the eventual product distribution as well as the overall rate constants.

2. Computational Methods

All of the electronic structure calculations were carried out using the GAUSSIAN98 and GAUSSIAN03 program packages.[13,14] The geometries of all of the reactants, products, intermediates, and transition states were optimized using hybrid density functional B3LYP method with the 6-311++G(d,p) basis set. Frequency calculations were performed at the same level to check whether the obtained stationary point was an isomer or a first-order transition state, and the reactants, intermediates, and products possessed all real frequencies, whereas transition states had one and only one imaginary frequency. Connections of the transition states between designated local minima were confirmed by intrinsic reaction coordinate (IRC) calculations at the B3LYP/6-311++G(d,p) level. Single-point calculations of all species were performed by applying the G3B3[15,16] scheme using the geometries and zero-point vibration energies calculated at the B3LYP/6-

* To whom correspondence should be addressed. Fax: +86-431-88498026. E-mail: yhdd@mail.jlu.edu.cn.
† Jilin University.
‡ Beijing Institute of Technology.

10.1021/jp709700u CCC: $40.75
Published on Web 05/14/2008

TABLE 1: Total (a.u.) and Relative Energies (kcal/mol) of the Reactants and Important Isomers, Products, and Transition States for the HCNO + CN Reaction at the G3B3//B3LYP/6-311++G(d,p) (in Normal), CCSD(T)/aug-cc-pVTZ//B3LYP/6-311++G(d,p)+ZPVE (in Italic), and G3B3//QCISD/6-311++G(d,p) (in Curly Brackets) Levels

species	G3B3//B3LYP/6-311++G(d,p)	species	G3B3//B3LYP/6-311++G(d,p)
R CN + HCNO	−261.1682212 (0.0)	**TSL1c/r1**	−261.2094406 (−25.9)
	−260.8813061 (0.0)		*−260.9257662 (−27.9)*
	{−261.1684976 (0.0)}		
L1c NCCHNO	−261.2761940 (−67.8)	**TSr1/P1**	−261.1913452 (−14.5)
	−260.9937026 (−70.5)		*−260.9080367 (−16.8)*
			{−261.1905535 (−13.8)}
L1t NCCHNO	−261.2764509 (−67.9)	**TSL1t/P2**	−261.1879313 (−12.4)
	−260.9938034 (−70.6)		*−260.8992713 (−11.3)*
r1 N-cCONCH	−261.2166564 (−30.4)	**TSL1c/L2c**	−261.1887752 (−12.9)
	−260.9350913 (−33.8)		*−260.9070927 (−16.2)*
P1 HCN + NCO	−261.3052371 (−86.0)	**P2** NCCNO + H	−261.1917229 (−14.7)
	−261.0198161 (−86.9)		*−260.9033057 (−13.8)*
	{−261.3028286 (−84.3)}		
P3 NCCN + OH	−261.2696889 (−63.7)	**P4** ^{3}HCCN + NO	−261.1820525 (−8.7)
	−260.9852431 (−65.2)		*−260.8997174 (−11.6)*
			{−261.1822282 (−8.6)}
L2c CNCHNO	−261.2417651 (−46.1)	**L3** NCCNOH	−261.2404365 (−45.3)
L4 OCNCHN	−261.3275185 (−100.0)	**r2** cCHNOCN	−261.2519357 (−52.5)
TSL1t/L3	−261.1828869 (−9.2)	**TSL3/P3**	−261.2316940 (−39.8)
TS L2c/r2	−261.2080072 (−25.0)	**TSr2/L4**	−261.2422241 (−46.4)
TSL4/P1	−261.2905282 (−76.7)		

311++G(d,p) and QCISD/6-311++G(d,p) (only for selected species) levels.[17] Finally, to test the reliability, the highly cost-expensive CCSD(T)/aug-cc-pVTZ single-point energy calculations were performed at the B3LYP/6-311++G(d,p) geometries for relevant species. To predict the dynamics, we applied the master equation method,[18,19] which is a powerful tool in calculating the time-dependent, temperature-dependent, and pressure-dependent kinetics of a multiple-channel and multiple-well chemical reaction system. The details of the master equation rate constant calculations are presented in the Supporting Information.

3. Results and Discussions

Table 1 lists the energy data of the reactants, most important isomers, products, and transition states at the G3B3//B3LYP/6-311++G(d,p) and CCSD(T)/aug-cc-pVTZ//B3LYP/6-311++G(d,p)+ZPVE levels. The structural parameters of the reactants, important products, intermediates, and transition states are shown in Figure 1. The schematic PES of this reaction at the G3B3//B3LYP/6-311++G(d,p) level is presented in Figure 2a,b. The total energy of the reactant **R** HCNO + CN is set as zero. Here, the symbol **Ln** means chainlike structures, and the symbol **rn** means cyclic structures (**n** is an Arabic numeral). The symbols **Lnc** and **Lnt** mean *cis*-**Ln** and *trans*-**Ln**. The symbol **TSx/y** is used to denote the transition state connecting the isomers **x** and **y**.

3.1. Entrance Channels. Four possible attack ways of CN radical on the HCNO molecule in entrance channels are considered as follows: (i) direct H abstraction to form **P11** HCN + CNO (−22.2) and **P13** HNC + CNO (−7.1) via **TSR/P11** (8.1) and via **TSR/P13** (17.9), respectively; (ii) C addition to form **L5** HCNOCN (−1.9) via **TSR/L5**(7.8); (iii) C addition to form **L1c** NCCHNO (−67.8) or **L1t** NCCHNO (−67.9) via a barrierless process (see the barrierless potential energy curves scanned at the G3B3//B3LYP/6-311++G(d,p) level in the Supporting Information); and (iv) N addition to form **L2c** CNCHNO (−46.1) via **TSR/L2c** (1.8). It is worth noting that **TSR/L2c** was located at the G3B3//UBH&HLYP/6-311++G(d,p) level. Although lots of attempts have been performed, we failed to locate it at the G3B3//B3LYP/6-311++G(d,p) level. The values, except **TSR/L2c** in process iv in parentheses, are G3B3 relative energies in kcal/mol with reference to **R** (0,0). It is obviously seen that C barrierless addition forming an intermediate **L1c** or **L1t** is thermodynamically and kinetically more favorable than other entrance pathways, which is consistent with the fact that most spin density concentrates on the C site (0.857e) of CN; therefore, the C site should be the most reactive site. Note that **L1c** and **L1t** can be interconverted to each other with the barriers around or less than 12 kcal/mol.

3.2. Isomerization and Dissociation. Starting from the most favorable entrance isomer **L1** NCCHNO, 11 possible reaction pathways are identified as follows: (i) ring closure leading to a four-membered ring **r1** N-cCONCH (−30.4); (ii) rearrangement leading to **L2c** CNCHNO (−46.1); (iii) H extrusion leading to **P2** NCCNO + H (−14.7); (iv) 1,3-H shift leading to **L3** NCCNOH (−45.3); (v) NO elimination leading to **P4** ^{3}HCCN + NO (−8.7); (vi) ring closure leading to a five-membered ring **r3** cCHNONC (−17.5); (vii) 1,2-H shift forming **L7** NCCNHO (−23.3); (viii) NC group shift forming **L8t** HCN(O)CN (−3.0); (ix) 1,2-H shift forming **L9** NCHCNO (−36.2); (x) 1,3-H shift forming **L6** HNCCNO (−35.3); and (xi) ring closure forming a four-membered ring **r5** O-cNNCCH (37.1). Processes vi−xi should have little contribution to the last product distribution due to the high energy of the intermediate or transition state; therefore, further transformation need not been considered. All species in the remaining five channels (i−v) are lower in energy than the reactant **R**, which should be of interest in combustion. However, their transformation and competitive mechanism are rather complicated. The main competitive channels deduced from Figure 2a are presented in Figure 2b. Their pathways are schematically written as follows:

$$\mathbf{L1} \rightarrow \mathbf{r1}\ \text{N-cCONCH} \rightarrow \mathbf{P1}\ \text{HCN} + \text{NCO} \quad \text{(I)}$$

$$\mathbf{L1} \rightarrow \mathbf{L2c}\ \text{CNCHNO} \rightarrow \mathbf{r2}\ \text{cCHNOCN} \rightarrow \mathbf{L4}\ \text{OCNCHN} \rightarrow \mathbf{P1}\ \text{HCN} + \text{NCO} \quad \text{(II)}$$

$$\mathbf{L1} \rightarrow \mathbf{P2}\ \text{NCCNO} + \text{H} \quad \text{(III)}$$

$$\mathbf{L1} \rightarrow \mathbf{L3}\ \text{NCCNOH} \rightarrow \mathbf{P3}\ \text{NCCN} + \text{OH} \quad \text{(IV)}$$

$$\mathbf{L1} \rightarrow \mathbf{P4}\ \text{HCCN} + \text{NO} \quad \text{(V)}$$

The rate-determining transition state **TSr1/P1** of path I, which leads to the product **P1** HCN + NCO (−86.0) via successive ring closure and concerted CC and NO bond rupture, is

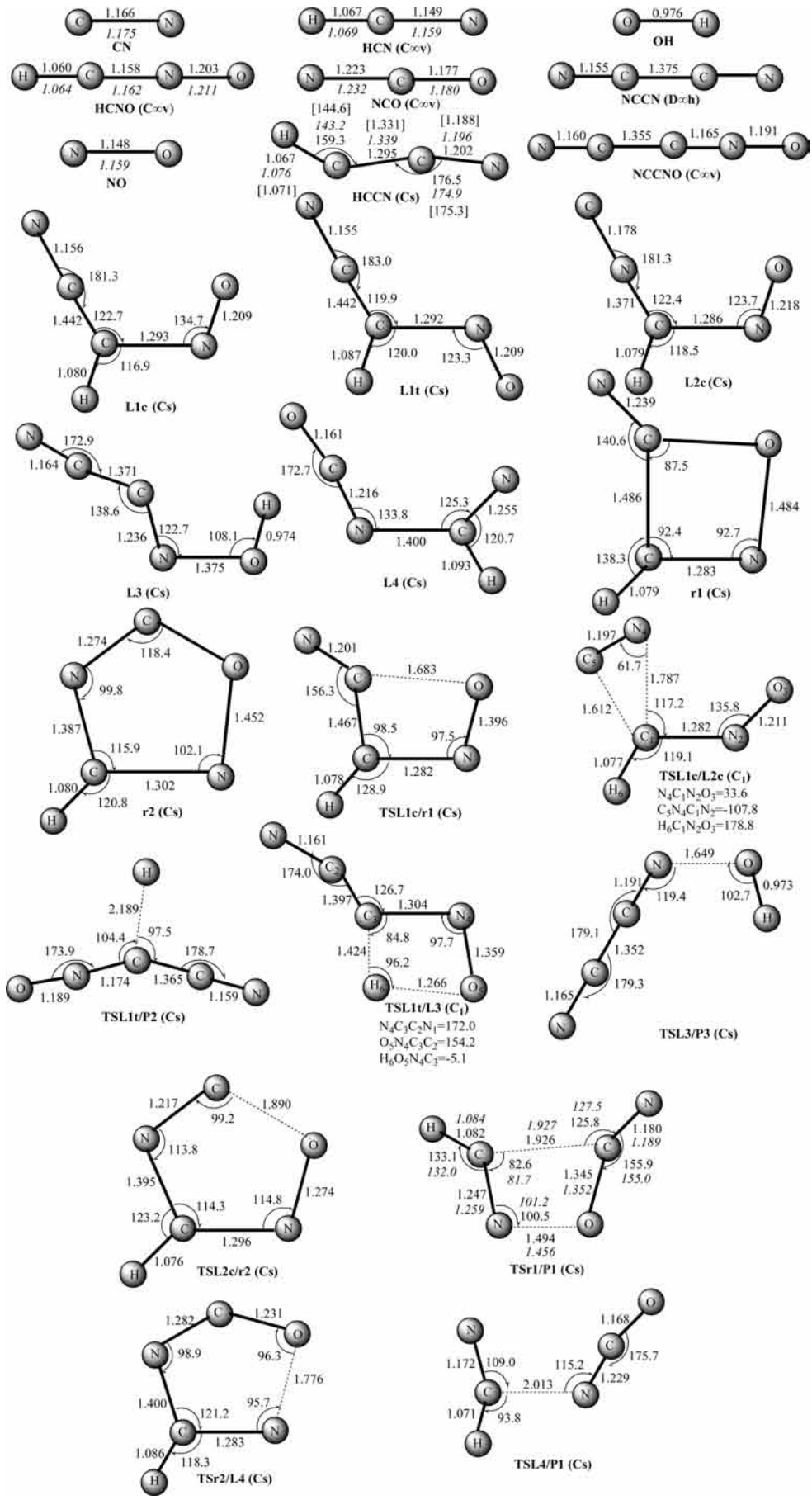

Figure 1. Optimized geometries of reactants and most important isomers, products, and transition states for the HCNO + CN reaction at the B3LYP/6-311++G(d,p), QCISD/6-311++G(d,p) (in italic), and CCSD(T)/cc-pV5Z[27] (in brackets) levels. Bond lengths are in Ångstroms, and angles are in degrees.

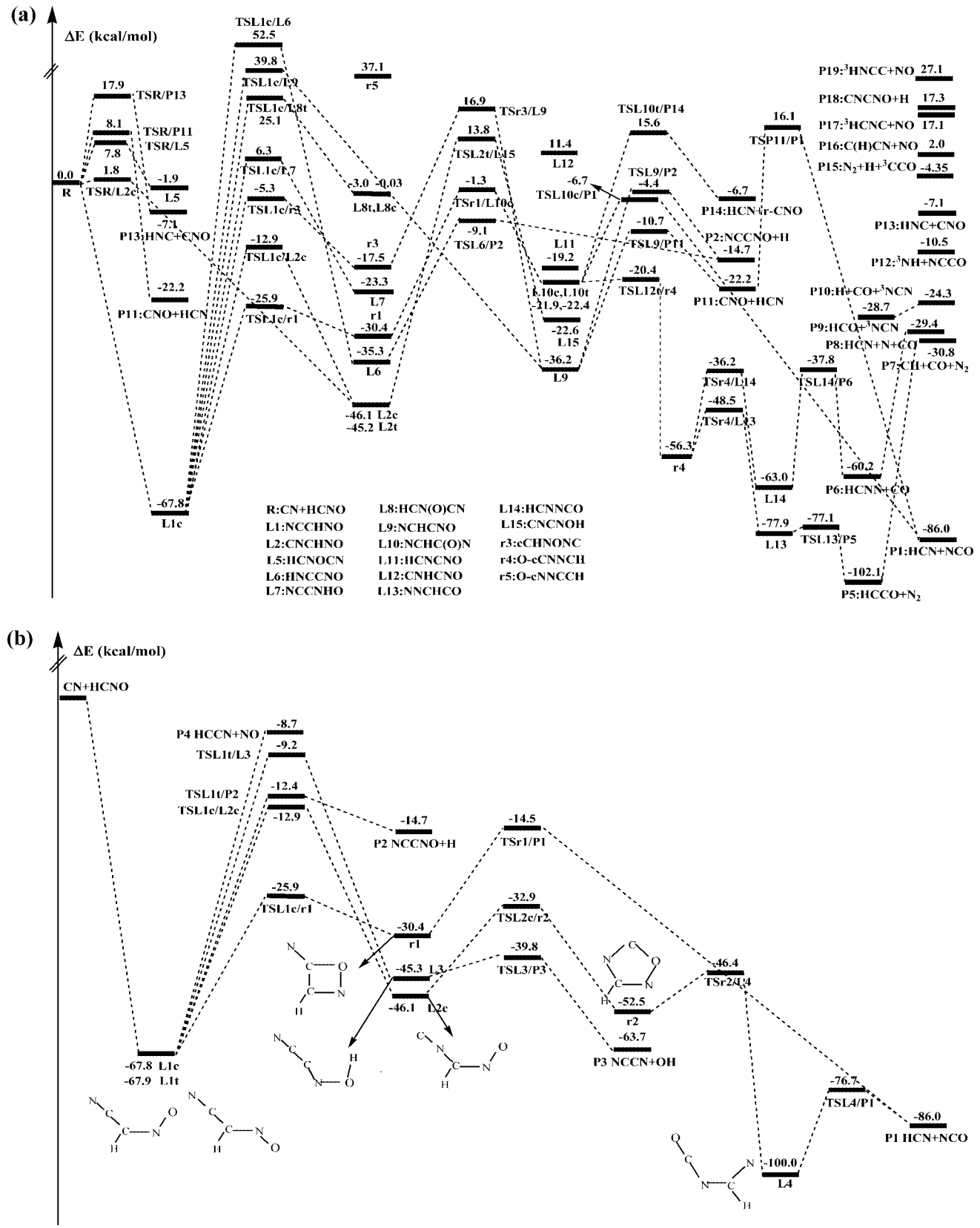

Figure 2. (a) Schematic PES of the HCNO + CN reaction at the G3B3//B3LYP/6-311++G(d,p) level showing various entrance channels and some conversion pathways starting from isomer **L1** NCCHNO. (b) Schematic PES of the HCNO + CN reaction at the G3B3//B3LYP/6-311++G(d,p) level showing the relevant important conversion pathways of isomer **L1** NCCHNO.

energetically lower than those in paths II (**TSL1c/L2c**), III (**TSL1t/P2**), and IV (**TSL1t/L3**) by 1.6, 2.1, and 5.3, respectively, and lower than product **P4** HCCN + NO in path V by 5.8 kcal/mol. Surely, the most competitive pathway is the formation of **P1** HCN + NCO via path I. Yet, the product **P4** HCCN + NO predicted in Feng et al.'s experiment[2] cannot compete with the formation of **P1** HCN + NCO due to its high energy in the product itself.

TABLE 2: Rate Constants (k in cm^3 Molecule^{-1} s^{-1} × 10^{10}) at Various Pressures (P in Torr) and Temperatures (T in K) from the Master Equation Rate Constant Calculations[a]

	Torr									
K	1	2	3	5	10	50	100	300	500	760
298	1.11 (1.07 ± 0.30)	1.11	1.11	1.11	1.11	1.11	1.11	1.11	1.12	1.12
330	1.51 (0.97 ± 0.26)	1.51	1.51	1.51	1.51	1.51	1.51	1.51	1.52	1.52
356	1.88 (0.91 ± 0.23)	1.88	1.88	1.88	1.88	1.88	1.88	1.88	1.89	1.89
388	2.38 (0.85 ± 0.21)	2.38	2.38	2.38	2.38	2.39	2.39	2.39	2.40	2.41
600	6.41	6.41	6.41	6.41	6.41	6.41	6.41	6.43	6.44	6.46
800	9.39	9.39	9.39	9.39	9.39	9.40	9.40	9.41	9.43	9.45
1000	10.72	10.72	10.72	10.72	10.72	10.72	10.72	10.73	10.74	10.76
1200	10.88	10.88	10.88	10.88	10.88	10.88	10.88	10.89	10.89	10.90
1500	10.32	10.32	10.32	10.32	10.32	10.32	10.32	10.32	10.32	10.33

[a] The experimental data by Feng et al. are presented in parentheses.[2]

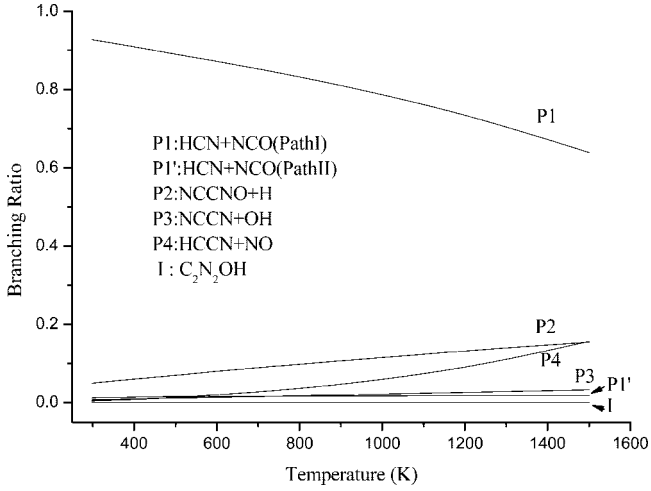

Figure 3. Branching ratios for the formation of **P1** HCN + NCO (path I), **P1′** HCN + NCO (path II), **P2** NCCNO + H, **P3** NCCN + OH, **P4** HCCN + NO, and **I** C_2N_2OH isomers at 1 Torr as a function of temperature.

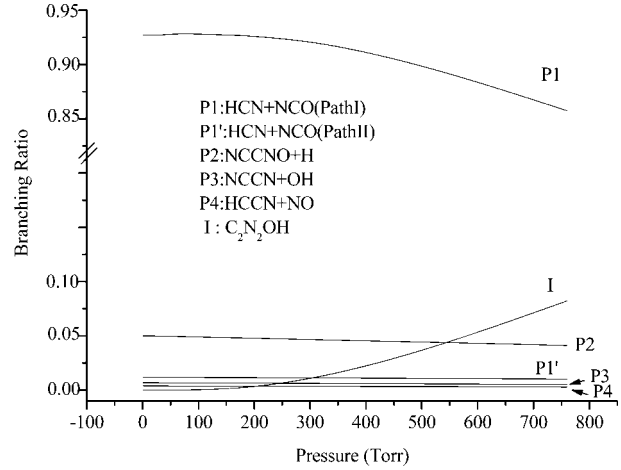

Figure 4. Branching ratios for the formation of **P1** HCN + NCO (path I), **P1′** HCN + NCO (path II), **P2** NCCNO + H, **P3** NCCN + OH, **P4** HCCN + NO, and **I** C_2N_2OH isomers at 298 K as a function of pressure.

3.3. Master Equation Rate Constant Calculation. For a deeper understanding and comparison of the HCNO + CN reaction with available experiments, we carried out master equation rate constant[16,17] calculations by making use of the G3B3//B3LYP/6-311++G(d,p) PES. Five channels with all species lower in energy than the reactant **R**, that is, paths I−V, are involved in the master equation rate constant calculation. Note that paths I−V are treated in a single master equation calculation. Because Feng et al.'s experimental study was limited to a very low pressure (1 Torr) and a very narrow temperature range (298−388 K),[2] we considered a wide range of temperatures (298−1500 K) and pressures (1−760 Torr) for a better kinetic understanding. The branching ratios of **P1** HCN + NCO (path I), **P1′** HCN + NCO (path II), **P2** NCCNO + H, **P3** NCCN + OH, **P4** HCCN + NO, and **I** C_2N_2OH isomers are plotted with respect to temperatures (298−1500 K at 1 Torr) (in Figure 3) and pressures (1−760 Torr at 298 K) (in Figure 4). Clearly, **P1** HCN + NCO is the predominant product, in agreement with the PES prediction. Yet, **P4** HCCN + NO, the major product proposed by Feng et al., has the negligibly small branching ratio (0.004 at 298 K) as compared to **P1** HCN + NCO (0.93 at 298 K). As the temperature increases, the branching ratio of **P1** gradually decreases, whereas the branching ratio of **P2** and **P4** keeps a gradual increase. The branching ratio of **P1′** and **P3** is always small. Moreover, in this low-pressure condition, the branching ratio of the intermediate isomer **I** C_2N_2OH is very small and negligible. As the pressure increases, the branching ratio of **P1** gradually decreases, while the branching ratio of **I** C_2N_2OH is gradually increased.

As shown in Table 2, our calculated rate constant values at 298, 330, 356, and 388 K are 1.11, 1.51, 1.88, and 2.38 × 10^{-10} cm^3 molecules^{-1} s^{-1}, respectively, which are comparable to the corresponding measured ones (1.07 ± 0.30), (0.97 ± 0.26), (0.91 ± 0.23), and (0.85 ± 0.21) × 10^{-10} cm^3 molecules^{-1} s^{-1} at 1 Torr by Feng et al.[2] The difference is that our calculations indicate a positive temperature dependence of rate constants, whereas Feng et al.'s measurement suggested a slight negative temperature dependence. Both our and Feng et al.'s results support no distinct pressure dependence effect of rate constants. Future laboratory study is much desirable for both the rate constant measurements and the product determination.

3.4. Reliability Assessment. Because our proposed mechanism for the title HCNO + CN reaction shows marked differences from the experimental result, it is highly desirable to assess the reliability of our calculated G3B3//B3LYP/6-311++G(d,p) results. The well-known "G3" series has been considered as a high-level and composite method, comprising a series of high-level single-point energy calculations, spin−orbital correction, and higher level correction.[15,16] For assessment of the accuracy of our calculated enthalpies of reaction, we considered 11 products (**P1**, **P3**−**P10**, **P12**, and **P15**), which lie lower than **R** HCNO + CN and whose experimental and accurate theoretical enthalpies of formation are available. As shown in Table 3, the agreement between the G3B3//B3LYP/6-311++G(d,p) results and the available experimental data is generally very good with the average deviation of 0.87 kcal/mol. In addition, we found from Table 3 that although the CCSD(T)/aug-cc-pVTZ//B3LYP/6-311++G(d,p)+ZPVE cal-

TABLE 3: Thermochemical Data (kcal/mol) from the Literature and Our Calculations [at the G3B3//B3LYP/6-311++G(d,p) Level and the CCSD(T)/aug-cc-pVTZ//B3LYP/6-311++G(d,p)+ZPVE Level] for Some Reaction Pathways

	$\Delta H_{r,298}^{\circ}$		
$\Delta H_{f,298}^{\circ}$ of reactants and products	experiment	G3B3//B3LYP/6-311++G(d,p)	CCSD(T)/aug-cc-pVTZ//B3LYP/6-311++G(d,p)+ZPVE
R: CN (104.9)[a] + HCNO (40.6)[b]			
P1: NCO (30.5)[c] + HCN (31.5)[a]	−83.5	−86.0	−87.0
P3: NCCN (73.3)[a] + OH (9.4)[a]	−62.8	−63.6	−65.2
P4: NO (21.6)[a] + ^{3}HCCN (115.6)[d]	−8.3	−8.7	−11.5
P5: HCCO (42.3)[e] + N_2 (0.0)[a]	−103.2	−102.2	−104.1
P6: CO (−26.4)[a] + HCNN (110.5)[f]	−61.4	−60.4	−62.5
P7: CH (142.5)[a] + CO (−26.4)[a] + N_2 (0.0)[a]	−29.4	−29.8	−34.6
P8: HCN (31.5)[a] + CO (−26.4)[a] + ^{4}N (113.5)[g]	−26.9	−28.5	−36.0
P9: HCO (10.0)[a] + ^{3}NCN (106.1)[f]	−29.4	−28.9	−31.3
P10: ^{3}NCN (106.1)[f] + CO (−26.4)[a] + H (52.6)[g]	−13.2	−13.4	−16.0
P12: ^{3}NH (85.2)[a] + NCCO (50.7)[h]	−9.6	−10.3	−12.3
P15: ^{3}CCO (91.1)[i] + N_2 (0.0)[a] + H (52.6)[g]	−1.8	−2.3	−6.0

[a] See ref 15. [b] See ref 20. [c] See ref 21. [d] See ref 22. [e] See ref 23. [f] See ref 24. [g] See ref 25. [h] See ref 26. [i] See ref 27.

culations are much more costly than the composite G3B3//B3LYP/6-311++G(d,p) ones, the former have larger deviations from the experimental data than the latter do, especially for those containing atomic fragments. This is understandable since the G3B3 method takes advantage of the assumption of additivity of various single-point energy calculations and inclusion of spin−orbital correction for atoms and higher level corrections.

For molecules with unique electronic structures, the calculated results may be largely influenced by the applied method and level. In particular, it has been shown that the energetics of ^{3}HCCN depend substantially on the calculated equilibrium geometries, the one-particle basis set, and the extent of electron correlation.[28] As shown in Figure 1, the bond distances and bond angles of ^{3}HCCN at the B3LYP/6-311++G(d,p) level seem to differ considerably from those at the costly QCISD/6-311++G(d,p) and CCSD(T)/cc-pV5Z[29] levels. Yet, the G3B3//B3LYP/6-311++G(d,p) reaction energy of **P4** ^{3}HCCN + NO (−8.7 kcal/mol) is very close to the G3B3//QCISD/6-311++G(d,p) value (−8.6 kcal/mol). For **P1** HCN + NCO and **TSr1/P1**, the agreement is also good with the deviation being 1.7 and 0.7 kcal/mol, respectively, as shown in Table 1. In all, for the title HCNO + CN reaction, the G3B3//B3LYP/6-311++G(d,p) computational scheme is able to provide reliable mechanistic information for the HCNO + CN reaction.

3.5. Chemical Implications. The above discussions based on the PES study and the master equation rate constant calculations both indicated that formation of **P1** HCN + NCO via path I is the major product channel, rather than **P4** ^{3}HCCN + NO (path V), which was recently proposed by Feng et al.[2] The detection of NO in the experiment might originate from other secondary reactions such as HCNO + NCO, for which NO + CO + HCN has been confirmed to be the major product by the recent experimental[4] and theoretical[5,6] studies.

The present results may have important implications. The reaction of CN radical with HCNO can predominantly lead to the product **P1** HCN + NCO in gas phase reaction. The HCN molecule is important in nitrogen recycle chemistry and is an important source for many N-related species.[30] Furthermore, the isocyanate radical NCO has received much attention. It is an important intermediate in combustion processes since this radical contributes to the conversion of fuel nitrogen to NO*x* and to the so-called "prompt" NO formation.[31] Thus, once the HCNO + CN reaction is initiated, its products might undertake sequential secondary reaction. This reinforces the significance of the title reaction in fuel-rich combustion processes.

4. Conclusions

In this paper, a combined quantum chemical and master equation rate constant calculation study is performed on the mechanism of the HCNO + CN reaction. The most favorable evolution pathway is barrierlessly forming addition product **L1** NCCHNO, followed by successive ring closure and concerted CC and NO bond rupture to generate the major product **P1** HCN + NCO. The formation of minor product **P2** NCCNO + H is less competitive in kinetics. However, the formation of **P4** ^{3}HCCN + NO, predicted as the only major product in recent experiment, is kinetically much less competitive. The master equation rate constant calculation shows that the title reaction has a positive temperature effect below 1200 K and no distinct pressure dependence effect, with a value of $k = 1.1 \times 10^{-10}$ cm^3 molecules^{-1} s^{-1} at 298 K. Future experimental reinvestigations are strongly desired to test the newly predicted mechanism for the HCNO + CN reaction. We hope that the present theoretical studies on the HCNO + CN reaction mechanism may be useful for understanding nitrogen combustion chemistry.

Acknowledgment. This work is supported by the National Natural Science Foundation of China (Nos. 20103003, 20573046, and 20773013), Excellent Young Teacher Foundation of the Ministry of Education of China, Excellent Young People Foundation of Jilin Province, and Program for New Century Excellent Talents in University (NCET). We thank the referees for their invaluable comments in improving the manuscript.

Supporting Information Available: Total and relative energies of all species at the B3LYP/6-311++G(d,p) and G3B3//B3LYP/6-311++G(d,p) levels (Table 1); vibrational frequencies and moments of inertia for reactants, important intermediates, and transition states predicted at the B3LYP/6-311++G(d,p) level of theory (Table 2); structural parameters for unimportant fragments, isomers, and transition states (Figure 1); potential energy curve for the formative process of the intermediate *cis*-**L1c** and *trans*-**L1t** at the G3B3//B3LYP/6-311++G(d,p) level (Figure 2a,b); and detailed theoretical method of the master equation rate constant calculation. This material is available free of charge via the Internet at http://pubs.acs.org.

References and Notes

(1) Miller, J. A.; Klippenstein, S. J.; Glarborg, P. *Combust. Flame* **2003**, *135*, 357.

(2) Feng, W. H.; Hershberger, J. F. *J. Phys. Chem. A* **2006**, *110*, 12184.
(3) Feng, W. H.; Meyer, J. P.; Hershberger, J. F. *J. Phys. Chem. A* **2006**, *110*, 4458.
(4) Feng, W. H.; Hershberger, J. F. *J. Phys. Chem. A* **2007**, *111*, 3831.
(5) Li, B. T.; Zhang, J.; Wu, H. S.; Sun, G. D. *J. Phys. Chem. A* **2007**, *111*, 7211.
(6) Zhang, W. C.; Du, B. N.; Feng, C. J. *Chem. Phys. Lett.* **2007**, *442*, 1.
(7) Zabardasti, A.; Solimannejad, M. *J. Mol. Struct.: THEOCHEM* **2007**, *810*, 73.
(8) Fenimore, C. P. *Symp. (Int.) Combust.* **1971**, *13*, 373.
(9) Haynes, B. S.; Iverach, D.; Kirov, N. Y. *Symp. (Int.) Combust.* **1974**, *15*, 1103.
(10) Fenimore, C. P. *Combust. Flame* **1972**, *19*, 289.
(11) Adamson, J. D.; DeSain, J. D.; Curl, R. F.; Glass, G. P. *J. Phys. Chem. A* **1997**, *101*, 864.
(12) Wei, Z. G.; Huang, X. R.; Sun, Y. B.; Sun, C. C. *Chem. J. Chin. Univ.* **2004**, *25*, 2112.
(13) Frisch, M. J.; Trucks, G. W.; Schlegel, H. B.; Scusera, G. E.; Robb, M. A.; Cheeseman, J. R.; Zakrzewski, V. G.; Montgomery, J. A., Jr.; Stratmann, R. E.; Burant, J. C.; Dapprich, S.; Millam, J. M.; Daniels, A. D.; Kudin, K. N.; Strain, M. C.; Farkas, O.; Tomasi, J.; Barone, V.; Cossi, M.; Cammi, R.; Mennucci, B.; Pomelli, C.; Adamo, C.; Clifford, S.; Ochterski, J.; Petersson, G. A.; Ayala, P. Y.; Cui, Q.; Morokuma, K.; Malick, D. K.; Rabuck, A. D.; Raghavachari, K.; Foresman, J. B.; Cioslowski, J.; Ortiz, J. V.; Stefanov, B. B.; Liu, G.; Liashenko, A.; Piskorz, P.; Komaromi, I.; Gomperts, R.; Martin, R. L.; Fox, D. J.; Keith, T.; Al-Laham, M. A.; Peng, C. Y.; Nanayakkara, A.; Gonzalez, C.; Challacombe, M.; Gill, P. M. W.; Johnson, B.; Chen, W.; Wong, M. W.; Andres, J. L.; Gonzalez, C.; Head-Gordon, M.; Replogle, E. S.; Pople, J. A. *Gaussian 98*, Revision A.6; Gaussian, Inc.: Pittsburgh, PA, 1998.
(14) Frisch, M. J.; Trucks, G. W.; Schlegel, H. B.; Scuseria, G. E.; Robb, M. A.; Cheeseman, J. R.; Montgomery, J. A., Jr.; Vreven, T.; Kudin, K. N.; Burant, J. C.; Millam, J. M.; Iyengar, S. S.; Tomasi, J.; Barone, V.; Mennucci, B.; Cossi, M.; Scalmani, G.; Rega, N.; Petersson, G. A.; Nakatsuji, H.; Hada, M.; Ehara, M.; Toyota, K.; Fukuda, R.; Hasegawa, J.; Ishida, M.; Nakajima, T.; Honda, Y.; Kitao, O.; Nakai, H.; Klene, M.; Li, X.; Knox, J. E.; Hratchian, H. P.; Cross, J. B.; Bakken, V.; Adamo, C.; Jaramillo, J.; Gomperts, R.; Stratmann, R. E.; Yazyev, O.; Austin, A. J.; Cammi, R.; Pomelli, C.; Ochterski, J. W.; Ayala, P. Y.; Morokuma, K.; Voth, G. A.; Salvador, P.; Dannenberg, J. J.; Zakrzewski, V. G.; Dapprich, S.; Daniels, A. D.; Strain, M. C.; Farkas, O.; Malick, D. K.; Rabuck, A. D.; Raghavachari, K.; Foresman, J. B.; Ortiz, J. V.; Cui, Q.; Baboul, A. G.; Clifford, S.; Cioslowski, J.; Stefanov, B. B.; Liu, G.; Liashenko, A.; Piskorz, P.; Komaromi, I.; Martin, R. L.; Fox, D. J.; Keith, T.; Al-Laham, M. A.; Peng, C. Y.; Nanayakkara, A.; Challacombe, M.; Gill, P. M. W.; Johnson, B.; Chen, W.; Wong, M. W.; Gonzalez, C.; Pople, J. A. *Gaussian 03*, Revision B.03; Gaussian, Inc.: Wallingford, CT, 2004.
(15) Curtiss, L. A.; Raghavachari, K.; Redfern, P. C.; Rassolov, V.; Pople, J. A. *J. Chem. Phys.* **1998**, *109*, 7764.
(16) Boboul, A. G.; Curtiss, L. A.; Redfern, P. C.; Raghavachari, K. J. *Chem. Phys.* **1999**, *110*, 7650.
(17) We should note that in the original G3 scheme that applies the DFT geometries, the B3LYP/6-31G(d) and zero-point energies were involved. The overall scheme is written as "G3//B3LYP". In our previous and present work on the G3 study of PESs of reactive systems, geometries at higher levels such as B3LYP/6-311++G(d.p) and QCISD/6-311++G(d,p) levels are used for better structural descriptions. The same scale factors as in the original G3//B3LYP scheme are still used. In this way, we denote the overall computational scheme as G3B3//B3LYP/6-311++G(d.p) and G3B3//QCISD/6-311++G(d.p) (if applied).
(18) (a) Klippenstein, S. J.; Miller, J. A. *J. Phys. Chem. A* **2002**, *106*, 9267. (b) Miller, J. A.; Klippenstein, S. J.; Robertson, S. H. *J. Phys. Chem. A* **2002**, *104*, 7525. (c) Pilling, M. J.; Robertson, S. H. *Annu. Rev. Phys. Chem.* **2003**, *54*, 245. (d) Frankcombe, T. J.; Smith, S. C. *J. Chem. Phys.* **2003**, *119*, 12741. (e) Gilbert, R. G.; Smith, S. C. *Theory of Unimolecular and Recombination Reactions*; Blackwell Scientific: Carlton, Australia, 1990. (f) Miller, J. A.; Klippenstein, S. J. *Int. J. Chem. Kinet.* **2001**, *33*, 654.
(19) Zhang, S. W.; Truong, T. N. VKLAB, version 1.0; University of Utah: Salt Lake City, UT, 2001.
(20) Schuurman, M. S.; Muir, S. R.; Allen, W. D.; Schaefer, H. F. *J. Chem. Phys.* **2004**, *120*, 11586.
(21) Cyr, D. R.; Continetti, R. E.; Metz, R. B.; Osborn, D. L.; Neumark, D. M. *J. Chem. Phys.* **1992**, *97*, 4937.
(22) Poutsma, J. C.; Upshaw, S. D.; Squires, R. R.; Wenthold, P. G. *J. Phys. Chem. A* **2002**, *106*, 1067.
(23) Osborn, D. L.; Mordaunt, D. H.; Choi, H.; Bise, R. T.; Neumark, D. M.; Rohlfing, C. M. *J. Chem. Phys.* **1997**, *106*, 10087.
(24) Clifford, E. P.; Wenthold, P. G.; Lineberger, W. C.; Petersson, G. A.; Broadus, K. M.; Kass, S. R.; Kato, S. J.; DePuy, C. H.; Bierbaum, V. M.; Ellison, G. B. *J. Phys. Chem. A* **1998**, *102*, 7100.
(25) Curtiss, L. A.; Raghavachari, K.; Redfern, P. C.; Pople, J. A. *J. Chem. Phys.* **1997**, *106*, 1063.
(26) Francisco, J. S.; Liu, R. F. *J. Chem. Phys.* **1997**, *107*, 3840.
(27) Choi, H.; Mordaunt, D. H.; Bise, R. T.; Taylor, T. R.; Neumark, D. M. *J. Chem. Phys.* **1998**, *108*, 4070.
(28) Francisco, J. S. *Chem. Phys. Lett.* **1994**, *230*, 372.
(29) Koput, J. *J. Phys. Chem. A* **2003**, *107*, 4717.
(30) Moskaleva, L. V.; Xia, W. S.; Lin, M. C. *Chem. Phys. Lett.* **2000**, *331*, 269.
(31) Miller, J. A.; Bowman, C. T. *Prog. Energy Combust. Sci.* **1989**, *15*, 287.

JP709700U